Elliptical high-order harmonic generation from H_2^+ driven by orthogonally polarized two-color laser fields

Xiao-Xin Huo ◉, Yun-He Xing, Tong Qi ◉, Yue Sun, Bo Li, Jun Zhang,[*] and Xue-Shen Liu[†]
Institute of Atomic and Molecular Physics, Jilin University, Changchun 130012, China

We theoretically investigate the elliptical high-order harmonic generation from the H_2^+ molecule driven by the orthogonally polarized two-color laser field by numerically solving the two-dimensional time-dependent Schrödinger equation. The results show that the odd-order harmonics in the x component and the even-order harmonics in the y component can be generated with the specific alignment angle $\theta = 0°$ for the different intensity ratios of the laser fields. The harmonic intensity distribution and ellipticity distribution at the different intensity ratios of the laser fields and the alignment angles differ significantly from each other. The result also shows that the ellipticity-tunable high-order harmonics can be generated through adjusting the intensity ratio of the laser fields and the alignment angles. Further analyses show that the amplitude ratio and the phase difference of the x and y components of the harmonics are the origin of the ellipticity of the harmonics in general. The two-center interference effect can also affect the ellipticity of the harmonics. The results show that the ellipticity of the harmonics can be used as a potential tool to probe the position of the minimum. The results we obtained can be useful for the optimization of elliptically polarized XUV radiation generation.

I. INTRODUCTION

High-order harmonic generation (HHG) is currently a hot research topic in strong field physics due to its extremely potential applications. The HHG can provide an effective way to generate the coherent attosecond pulse [1] and can be used to probe the dynamic processes of multielectrons [2,3]. It is also an ideal light source to obtain XUV bands and x rays [4]. The HHG as a nonlinear process can be successfully described by the semiclassical three-step model [5]. First, the electron is ionized into the continuum in the laser field through the tunneling. Then, the electron continues to be accelerated in the laser field. Finally, the electron recombines with the parent ion and emits the high-energy photon which is called the HHG. The typical harmonic spectrum has an obvious characteristic: it decreases rapidly in low order, then exhibits a plateau, and ends up with a sharp cutoff. The cutoff energy is expressed as $E_{\text{cutoff}} = I_p + 3.17U_p$, where $U_p = \frac{E_0^2}{4\omega_0^2}$ (E_0 is the amplitude of the laser field and ω_0 is the frequency of the laser field) is the ponderomotive energy and I_p is the ionization energy.

The influence of the intensity ratio of the two-color laser field on the HHG has been extensively investigated. The interaction between the HHG from current-carrying orbitals can be affected by adjusting the relative intensity ratio of the laser fields [6]. By changing the intensity ratio of the laser fields, the cutoff energy of the harmonic spectrum can be affected [7,8] and the harmonic intensity will increase as the intensity ratio increases [9].

In recent years, the elliptical HHG is of interest to the optics community. The investigations of the ellipticity of the HHG driven by linearly [10,11], circularly [12,13], elliptically [14], and orthogonally [15–17] polarized laser pulses have been a hot issue in experiment and theory. The dependence of the ellipticity can be attributed to the different HHG route, excited state, harmonic intensity, and harmonic phase [10,18–23]. Not only the crossing angle between the laser fields [9,24] but the alignment angle also has a significant effect on the ellipticity. For example, Habibović *et al.* [16] investigated the ellipticity from the N_2 molecule as a function of the molecular orientation and found that the harmonic ellipticity changes rapidly for those orientations for which the total ionization rate exhibits minima by analyzing the quantum orbits. Mairesse *et al.* [25] investigated the ellipticity of HHG from the N_2 molecule for different alignment angles θ driven by a linearly polarized laser field. The results demonstrated that the maximum ellipticity occurs around $\theta = 50°$–$60°$ and the ellipticity has a larger value near the cutoff at low laser intensity. Li *et al.* [26] found that the ellipticity of the harmonics from the H_2^+ molecule driven by the bichromatic counter-rotating circularly polarized (BCCP) laser field can be controlled by changing the molecular alignment angle. The results demonstrated that there is a critical angle at which the ellipticity of each harmonic is equal. Dong *et al.* [27] investigated the HHG from the H_2^+ molecule driven by a linearly polarized laser field and found that the orientation angle has a great influence on the ellipticity of low-order harmonics (LOHs) and the change in ellipticity is significant for different harmonic orders.

In addition, the molecular two-center interference effect also makes a significant contribution to the ellipticity of the harmonics. An important characteristic of the harmonic spectrum affected by the two-center interference effect is the

---

*[*]jluzjun@jlu.edu.cn
[†]liuxs@jlu.edu.cn

minimum, which was put forward by Lein *et al*. [28,29] in theory. The minimum occurs due to the two-center interference of the molecules, and the interference of the contributions from two different nuclei in the molecule can result in the suppression of the harmonics [30–34]. In addition, Das *et al*. [35] chose an appropriate driving-field intensity to avoid the effects of two-center interference and also found that the harmonics are suppressed when the angle of the molecular axis with respect to the main polarization axis of the laser field is 0, $\pi/2$, π, $3\pi/2$ for the O_2 molecule driven by an orthogonally polarized two-color (OTC) laser field. Son *et al*. [19] investigated the HHG from the H_2^+ molecule driven by a linearly polarized laser field by *ab initio* calculations and demonstrated that the molecular two-center interference effects can produce the high ellipticity. Kim *et al*. [36] demonstrated that the ellipticity of the harmonics around the interference minima region can reach the maximum from the H_2^+ and the H_2 molecules driven by a linearly polarized laser field. Zwan *et al*. [37] observed the significant ellipticity of the harmonics around the interference minimum, and it was attributed to the Coulomb effects.

In this paper, we investigate the ellipticity of the harmonics from the aligned H_2^+ molecule driven by the OTC laser pulse through numerically solving the two-dimensional (2D) time-dependent Schrödinger equation (TDSE). Our results show that the odd-order harmonics in the x component and the even-order harmonics in the y component can be generated by the OTC laser field with the alignment angle $\theta = 0°$. The ellipticity-tunable high-order harmonics can be generated through adjusting the intensity ratio of the laser fields and the alignment angles. The phase difference of the x and y components of the harmonics with $\theta = -54°$ is investigated to explain the physical mechanism of the ellipticity. The harmonic intensity distribution can also be used to illustrate the ellipticity distribution of the harmonics. The harmonic spectrum generated with and without interference effects is investigated, which is used to demonstrate the dependence of the ellipticity.

II. THEORETICAL METHODS

We investigate the HHG from the H_2^+ molecule by numerically solving the 2D TDSE. The 2D TDSE in dipole approximation for the H_2^+ molecule can be given by

$$\frac{\partial \psi(x, y, t)}{\partial t} = \left[\frac{P_x^2 + P_y^2}{2} + V_C(x, y) + x E_x(t) + y E_y(t) \right] \psi(x, y, t), \quad (1)$$

where $\vec{P} = P_x \hat{e}_x + P_y \hat{e}_y$ is the momentum operator, $\hat{e}_x$ and $\hat{e}_y$ are the unit vectors in the x and y directions, respectively,

$$V_C(x, y) = -\frac{1}{\sqrt{\left(x - \frac{R}{2}\cos\theta\right)^2 + \left(y - \frac{R}{2}\sin\theta\right)^2 + a^2}} - \frac{1}{\sqrt{\left(x + \frac{R}{2}\cos\theta\right)^2 + \left(y + \frac{R}{2}\sin\theta\right)^2 + a^2}} \quad (2)$$

is the soft-core Coulomb potential of diatomic molecular ion, where θ is the alignment angle between the molecular axis and the x axis, $R = 2.0$ a.u. is the equilibrium internuclear distance, and $a = 0.735$ is the soft-core parameter, which corresponds to the ionization potential $I_p = 1.09$ a.u. of the H_2^+ molecule [26].

The external electric field is an OTC laser field, which consists of a fundamental field $E_x(t)$ and a second-harmonic field $E_y(t)$. It is expressed as

$$\begin{aligned} E(t) &= \vec{E}_x(t) + \vec{E}_y(t) \\ &= E_0 f(t)[\hat{e}_x \sin(\omega_0 t) + \gamma \hat{e}_y \sin(2\omega_0 t)], \quad (3) \end{aligned}$$

where $f(t)$ is a trapezoidal envelope of the laser pulse with a total duration of three optical cycles and linear ramps of one cycle [38], E_0 is the amplitude of the laser field, ω_0 is the frequency of the fundamental field, and γ is the laser intensity ratio, which can reflect the relative amplitude of the two laser fields. We use the split operator method to solve the TDSE. The time step is 0.05 a.u. and the spatial integration grid size is 409.6 a.u. The mask function has been adopted for suppressing the reflection from boundaries [39].

The dipole acceleration can be given by the Ehrenfest theorem

$$\begin{aligned} d_x(t) &= \langle \psi(x, y, t) | - \frac{\partial V(x, y)}{\partial x} + E_x(t) | \psi(x, y, t) \rangle, \\ d_y(t) &= \langle \psi(x, y, t) | - \frac{\partial V(x, y)}{\partial y} + E_y(t) | \psi(x, y, t) \rangle. \end{aligned} \quad (4)$$

By simulating the modulus squared of the Fourier transformation of dipole acceleration, the HHG spectrum can be expressed as

$$\begin{aligned} F_x(\omega) &= \left| \frac{1}{T - t_0} \int_{t_0}^{T} d_x(t) e^{-i\omega t} dt \right|^2, \\ F_y(\omega) &= \left| \frac{1}{T - t_0} \int_{t_0}^{T} d_y(t) e^{-i\omega t} dt \right|^2, \end{aligned} \quad (5)$$

where t_0 is the initial moment and T is the final moment. The ellipticity of the harmonics can be obtained from

$$\varepsilon = \frac{(|a_+| - |a_-|)}{(|a_+| + |a_-|)}, \quad (6)$$

where $a_\pm = \frac{1}{\sqrt{2}}(a_x \pm i a_y)$, with a_x and a_y being the x and y components of the dipole acceleration in the frequency domain, respectively [23]. The $\varepsilon = 0$, $0 < \varepsilon < 1$, and $\varepsilon = 1$ correspond to the linearly, elliptically, and circularly polarized harmonics, respectively. In addition, according to Eq. (6), we can obtain another expression of the ellipticity by complex derivation. It can be expressed as

$$\varepsilon = \sqrt{\frac{1 + r^2 - \sqrt{1 + r^4 + 2r^2 \cos 2\delta}}{1 + r^2 + \sqrt{1 + r^4 + 2r^2 \cos 2\delta}}}. \quad (7)$$

It is consistent with the expression of the ellipticity of Eq. (3) in Ref. [19]. Where $r = |a_y|/|a_x|$, $\delta = \phi_y - \phi_x$ is the phase difference of the x and y components of the harmonics. $\phi_{x,y}(\omega) = \arg[a_{x,y}(\omega)]$ and $a_{x,y}(\omega) = \int_{-\infty}^{\infty} d_{x,y}(t) e^{-i\omega t} dt$ [19]. The expressions of Eq. (6) and Eq. (7) are consistent, which
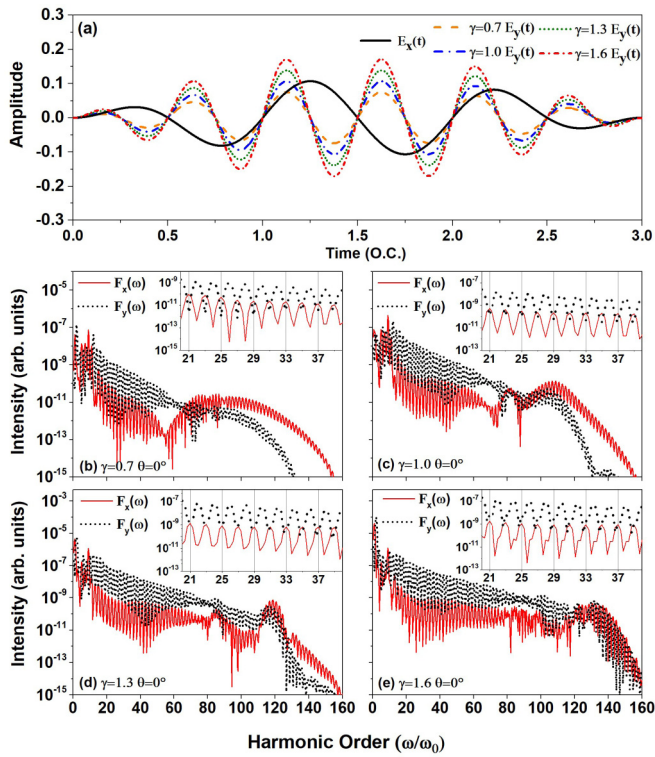
FIG. 1. (a) Electric field of the OTC laser pulse for four different intensity ratios $\gamma = 0.7, 1.0, 1.3, 1.6$, where $E_x(t)$ represents the fundamental field and $E_y(t)$ represents the second-harmonic field. The harmonic spectrum generated by the OTC laser field for four intensity ratios (b) $\gamma = 0.7$, (c) $\gamma = 1.0$, (d) $\gamma = 1.3$, and (e) $\gamma = 1.6$ with $\theta = 0°$. The red solid and black dotted lines correspond to the x and y components of the generated harmonic spectrum, respectively. The insets show the detailed harmonic spectrum from 20th to 40th order.

have been widely used for the investigation of the ellipticity of the HHG, such as in Refs. [10,19,23,26,27].

III. RESULTS AND DISCUSSIONS

Figure 1 presents the electric field of the OTC laser pulse and the x and y components of the harmonic spectrum driven by the OTC laser pulse with the alignment angle $\theta = 0°$ for four intensity ratios $\gamma = 0.7, 1.0, 1.3, 1.6$, respectively. The laser intensity $I_0 = 4 \times 10^{14}$ W/cm^2 ($E_0 = 0.10676$ a.u.) and the laser frequency $\omega_0 = 0.043$ a.u. ($\lambda = 1064$ nm). The insets in the upper right corner of Figs. 1(b)–1(e) show the detailed harmonic spectrum from 20th to 40th order.

Figure 1(a) shows the fundamental field $E_x(t)$ along x direction and the second-harmonic field $E_y(t)$ along y direction for four different intensity ratios $\gamma = 0.7, 1.0, 1.3, 1.6$. The intensity of the laser field along x direction remains unchanged and the intensity of the laser field along y direction gradually increases with the increase of the intensity ratio of the laser fields.

Figures 1(b)–1(e) present the harmonic spectra with $\gamma = 0.7, 1.0, 1.3, 1.6$, which show that the harmonic intensities increase gradually and the cutoff positions are extended with the increase of the intensity ratio of the laser fields. It

indicates that the harmonic intensity can be controlled by the intensity ratio of the two laser fields. There is a cross point of the x and y components of the harmonics, which moves to the higher order of the harmonics with the increase of the intensity ratio of the laser fields. The intensity in the y component of the harmonics is higher than that in the x component of the harmonics below the cross point. However, a reversed result is observed above the cross point. The minimum of the x component of the harmonics before the cross point can be found, which moves to the higher order of the harmonics with the increase of the intensity ratios. The intensity in the y component of the harmonics before the cross point is stronger than that in the x component of the harmonics, which leads to the disappearance of the minimum of the total harmonic spectrum (we do not show the total harmonics in this paper). In Ref. [36], Kim et al. investigated the harmonics of the H$_2^+$ and the H$_2$ molecules driven by a linearly polarized laser field and found that the minimum disappears if the y component of the harmonics plays a dominant role. Our result is consistent with that illustrated in Ref. [36]. We also find that the odd-order harmonics in the x component are produced and the even-order harmonics in the y component are produced with $\theta = 0°$, which can be seen clearly in the insets in Figs. 1(b)–1(e). The insets in Figs. 1(b)–1(e) also show that varying the intensity ratio of the laser fields can change the harmonic intensity, but it does not change the mechanism of the parity of the x and y components of the harmonics with the specific alignment angle $\theta = 0°$.

To illustrate the physical mechanism of the odd- and even-order harmonics in the insets in Figs. 1(b)–1(e), we investigate the harmonics driven by the linearly polarized laser field along x direction (at frequency ω_0 field) and along y direction (at frequency $2\omega_0$ field) (we do not show the harmonic spectrum here). We find that only the odd-order harmonics are generated at both frequency ω_0 and $2\omega_0$ fields. This means that the even-order harmonics at frequency ω_0 field are the odd-order harmonics at frequency $2\omega_0$ field.

The emission mechanism can be explained by the quantum transition. For frequency ω_0 field, according to the conservation of angular momentum, if m left-handed photons are absorbed, $m \pm 1$ right-handed photons must be absorbed and thus the radiated photon is $2m \pm 1$, $m = 0, 1, 2, 3, \ldots$ (the harmonics driven by the single-color contribution of frequency ω_0 field), which means that an odd multiple of photons are radiated, resulting in the odd-order harmonic generation. For frequency $2\omega_0$ field, the $4m \pm 2$, $m = 0, 1, 2, 3, \ldots$ order harmonics can be generated (the harmonics driven by the single-color contribution of frequency $2\omega_0$ field). But, from Figs. 1(b)–1(e), we find that the $4m \pm 4$, $m = 0, 1, 2, 3, \ldots$ order harmonics along y direction can also be generated driven by the OTC laser field (we think that the harmonics are generated by frequency mixing ω_0 and $2\omega_0$ field). According to the selection rules, $\Omega = n_1\omega_1 + n_2\omega_2$, $n_1 + n_2$ is an odd integer. n_1 represents the number of photons absorbed from ω_1 field and n_2 represents the number of photons absorbed from ω_2 field ($\omega_1 = \omega_0$, $\omega_2 = 2\omega_0$). In the following, we will use the notation (n_1, n_2) to represent the number of photons absorbed.

For example, for 20th, 28th, 32th, and 40th order harmonics, (6,7), (10,9), (10,11), and (14,13) pairs can contribute to the generation of the harmonics, respectively. Of course, it
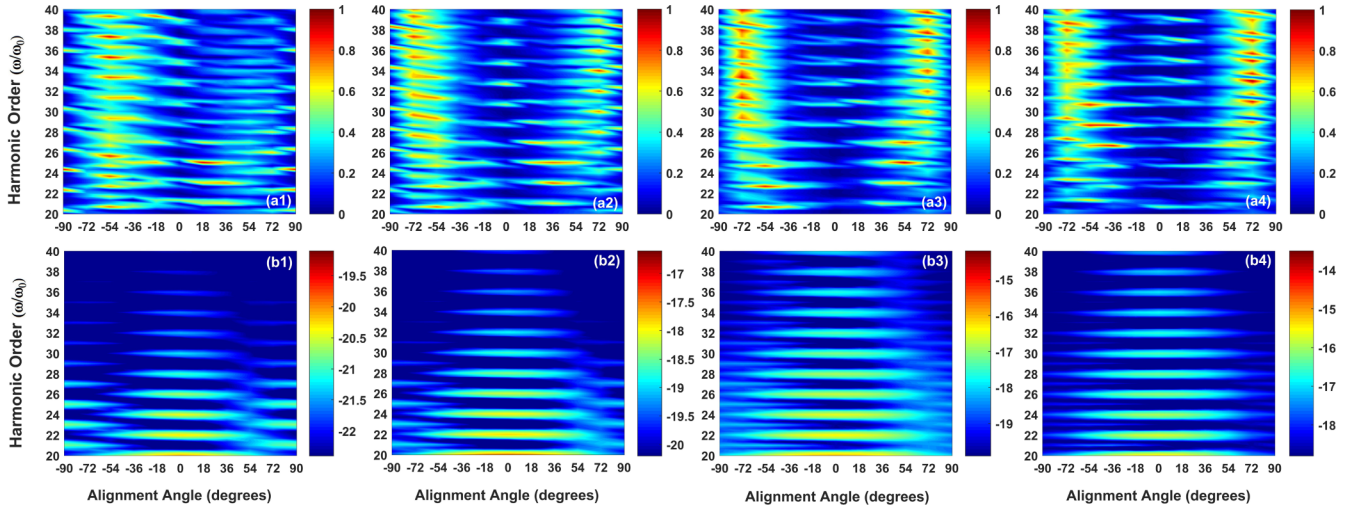
FIG. 2. Ellipticity distribution (a1)–(a4) and intensity distribution (b1)–(b4) of the HHG versus harmonic orders and alignment angles with different intensity ratios: (a1),(b1) $\gamma = 0.7$; (a2),(b2) $\gamma = 1.0$; (a3),(b3) $\gamma = 1.3$; (a4),(b4) $\gamma = 1.6$.

is possible that different (n_1, n_2) pairs can contribute to the emission of the given harmonics. Thus other pairs are also very likely to contribute to the total emission for 20th, 28th, 32th, and 40th order harmonics. For 24th and 36th order harmonics, (10,7), (6,9), etc. and (14,11), (10,13), etc. are likely to contribute to the generation of the harmonics, respectively. There is a more detailed analysis in Refs. [24,40–43].

Figures 2(a1)–2(a4) show the ellipticity distribution of the HHG versus harmonic orders and alignment angles for four different intensity ratios. For $\gamma = 0.7$, Fig. 2(a1) shows that the large ellipticities of the harmonics are generated around $\theta = -54°$ from 21st to 39th order and around $\theta = 18°$ from 21st to 27th order. For $\gamma = 1.0$, Fig. 2(a2) shows that the large ellipticities of the harmonics are generated around $\theta = -54°$ and $\theta = 36°$ from 21st to 27th order, and around $\theta = \pm 72°$ above 27th order. For $\gamma = 1.3, 1.6$, Figs. 2(a3)–2(a4) show that the large ellipticities of the harmonics are generated around $\theta = \pm 54°$ from 21st to 27th order, and around $\theta = \pm 72°$ above 27th order, where 21st and 27th order harmonics are close to the ionization threshold ($n = I_p/\omega_0 = 1.095/0.043 \approx 25$).

Figures 2(a1)–2(a4) show that the ellipticity is relatively small around $\theta = 0°$ compared to that of other alignment angles. The ellipticity gradually increases as the harmonic order increases around $\theta = 0°$ for the cases of four intensity ratios. The ellipticity of the odd- and even-order harmonics are comparable around $\theta = 72°$ from 31st to 40th order for $\gamma = 1.6$. This means that the ellipticity-tunable high-order harmonics can be generated through adjusting the intensity ratio of the laser fields and the alignment angles, which facilitates the synthesis of attosecond pulse with high degree of the ellipticity [9].

To illustrate the physical mechanism of the ellipticity distribution of the harmonics, Figs. 2(b1)–2(b4) show the harmonic intensity distribution versus harmonic orders and alignment angles for four different intensity ratios $\gamma = 0.7, 1.0, 1.3, 1.6$, respectively. It is illustrated that the positions of the maximal ellipticity indicate the positions of the harmonic intensity minima [44]. From Figs. 2(b1)–2(b4), we

can find that the harmonic intensity minimum occurs around $\theta = \pm 54°$ ($\gamma = 0.7$), $\theta = \pm 72°$ ($\gamma = 1.0, 1.3, 1.6$), which are in good agreement with the angles of the large ellipticity distribution as shown in Figs. 2(a1)–2(a4). We can also see that the harmonic intensity around $\theta = 0°$ is relatively strong compared to that of the other alignment angles and gradually decreases as the harmonic order increases, which is consistent with the ellipticity distribution as shown in Figs. 2(a1)–2(a4).

In order to further illustrate the physical mechanism of the ellipticity of the HHG, we show the ellipticity of the odd- and even-order harmonics with $\theta = 0°$ and $\theta = -54°$ for the different intensity ratios, as shown in Fig. 3.

From Fig. 3(a), for $\theta = 0°$, one can see that the ellipticity of the even-order harmonics are extremely small, and the ellipticity of the odd-order harmonics decreases first and then increases with the increase of the harmonic order from 21th to 39th order. With the increase of the intensity ratio of the laser fields, the ellipticity of the high-order harmonics becomes smaller from 29th to 39th order. In Ref. [6], Wang *et al.* investigated the ellipticity of the harmonics from polyatomic molecules driven by the BCCP laser field and found that, as the intensity of the second harmonic gets larger, the absolute values of the ellipticity get smaller. Our result is the same as that described in Ref. [6]. It also shows the small ellipticity near 23rd order for $\gamma = 0.7, 1.6$ and 25th and 27th orders for $\gamma = 1.0$ and $\gamma = 1.3$. The 23rd, 25th, and 27th orders are near to the ionization threshold. In Ref. [27], Dong *et al.* investigated the ellipticity of the LOHs driven by a linearly polarized laser field and found that the harmonics which are near to the ionization threshold show the small ellipticity. Our result is similar to that illustrated in Ref. [27].

However, the ellipticity of the odd-order harmonics with $\theta = 0°$ can be obtained as shown in Fig. 3(a), but the odd-order harmonics along y direction are not generated as shown in Figs. 1(b)–1(e). It is a specific case for $\theta = 0°$ to illustrate the ellipticity. In order to obtain a general conclusion, we choose $\theta = -54°$ to investigate the ellipticity further.

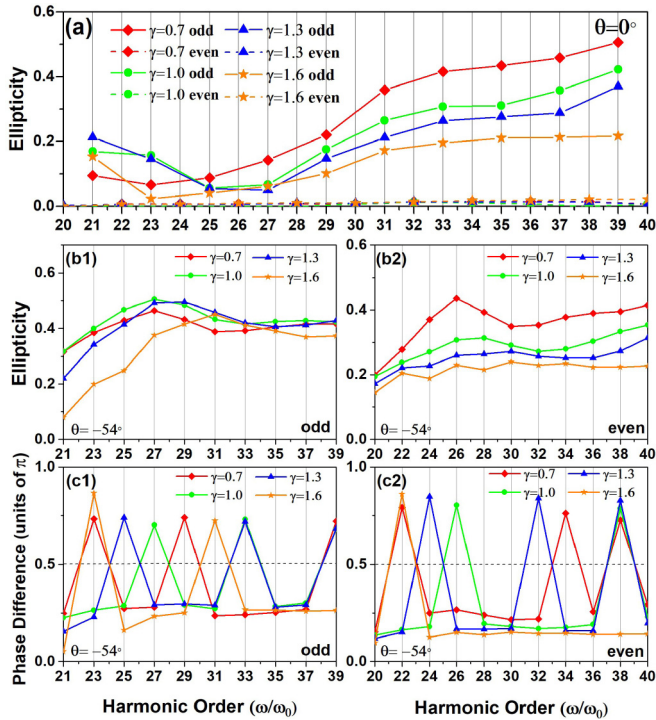For $\theta = -54°$, we show the ellipticity of the odd- and even-order harmonics, respectively, as shown in

FIG. 3. (a) Ellipticity of the odd- and even-order harmonics with $\theta = 0°$. (b1),(b2) The ellipticity of the odd- and even-order harmonics with $\theta = -54°$. (c1),(c2) The phase difference of the x and y components of the odd- and even-order harmonics with $\theta = -54°$ driven by the OTC laser field for different intensity ratios.

Figs. 3(b1) and 3(b2). We can find that the odd- and even-order harmonics can all generate the higher ellipticity and the ellipticity first reaches a maximum and then decreases, which is different from the ellipticity of the odd- and even-order harmonics with $\theta = 0°$. The orders corresponding to the maximum values are all near to the ionization threshold. From Fig. 3(b2), we can see that the ellipticity of the even-order harmonics with $\gamma = 0.7$ is the largest and it is the smallest with $\gamma = 1.6$. For $\theta = -54°$, the larger ellipticity can be obtained and both the odd- and even-order harmonics can be generated along x and y direction [here we do not show the harmonic spectrum with $\gamma = 0.7, 1.0, 1.3$, and the harmonic spectrum with $\gamma = 1.6$ is shown in Fig. 5(c)], which can illustrate the physical mechanism of the ellipticity in general.

In order to illustrate the ellipticity distribution of the harmonics, we investigate the phase difference of the x and y components of the harmonics [19]. In Figs. 3(c1) and 3(c2), we show the phase difference of the x and y components of the odd- and even-order harmonics with $\theta = -54°$, respectively. From the expression of the ellipticity of Eq. (7), we can see that the ellipticity has a strong dependence on the amplitude ratio and the phase difference of the x and y components of the harmonics. We can consider the following three cases from Eq. (7).

Case (1): if the phase difference of the x and y components of the harmonics is $\delta = 0$ or $\pm\pi$, then $\varepsilon = 0$ and the harmonics are completely linearly polarized.

Case (2): if the phase difference of the x and y components of the harmonics is $\pm\pi/2$ and the x and y components of

the harmonics have the same amplitude, then $\varepsilon = 1$ and the harmonics are circularly polarized.

Case (3): if the amplitude of the x and y components of the harmonics is different or the phase difference of the x and y components of the harmonics is not 0, $\pm\pi$, or $\pm\pi/2$, then $0 < \varepsilon < 1$ and the harmonics are elliptically polarized.

Thus, to achieve the high ellipticity, the following two cases should be satisfied [19]: (i) the amplitudes of the x and y components of the harmonics are comparable and (ii) their phase difference is around $\pm\pi/2$. If the phase difference is around 0 or $\pm\pi$, the ellipticity is small.

From Fig. 3(c2), we can see that the phase difference of the even-order harmonics with $\theta = -54°$ is closest to $\pi/2$ for $\gamma = 0.7$ and farthest away from $\pi/2$ for $\gamma = 1.6$, which correspond to the largest and the smallest ellipticity as shown in Fig. 3(b2).

We take $\gamma = 0.7$ as an example to illustrate the ellipticity. For the odd-order harmonics, Fig. 3(c1) shows that the phase difference with $\gamma = 0.7$ is the closest to $\pi/2$ first and then becomes the farthest away from $\pi/2$, which corresponds to the fact that the ellipticity first increases and then decreases, as shown in Fig. 3(b1). For the even-order harmonics, Fig. 3(c2) shows that the phase difference with $\gamma = 0.7$ is closer to $\pi/2$ from 20th to 26th order, and becomes farther away from $\pi/2$ from 26th to 30th, and then becomes closer to $\pi/2$ again for 30th to 40th order, which corresponds to the fact that the ellipticity of the even-order harmonics with $\gamma = 0.7$ first increases, then decreases, and then increases again, as shown in Fig. 3(b2). Other situations are consistent with this analysis.

Figure 4 shows the angular distribution of the ellipticity for 25th and 30th order harmonics with $\gamma = 0.7, 1.0, 1.3, 1.6$, respectively. Figures 4(a1)–4(a4) show that the maximum ellipticity occurs around $\theta = 36°, -54°$ ($\gamma = 0.7$), $\theta = 46°, -54°$ ($\gamma = 1.0$), and $\theta = \pm54°$ ($\gamma = 1.3, 1.6$) for 25th order harmonic. Figures 4(b1)–4(b4) show that the maximum ellipticity occurs around $\theta = \pm72°$ ($\gamma = 0.7, 1.0, 1.3, 1.6$) for 30th order harmonic. The angles of the maximum ellipticity distribution are centrosymmetric for each case. It can be seen that the polarization directions of the odd- and even-order harmonics are different. In Ref. [9], Zhai *et al.* investigated the influence of the crossing angle between the two laser fields on the ellipticity driven by cross-linearly polarized two-color field experimentally and the result showed that the odd- and even-order harmonics have different polarization directions. The results in our paper are consistent with that illustrated in Ref. [9].

The pointing angles of the ellipticity distribution of the same order are almost consistent for different intensity ratios, which means that the angular distribution of the ellipticity is insensitive to the intensity ratio at particular harmonic order. This is because the below-threshold harmonic generation mechanism is multiphoton ionization, due to the fact that 25th and 30th order harmonics are close to the ionization threshold; it is not sensitive to the changing of the intensity ratio of the laser fields.

In addition, we also investigate the angular distribution of the ellipticity of 13rd, 18th, 33rd, 38th, 43rd, 48th, 53rd, and 58th harmonics and we find that the difference in the pointing angle of the ellipticity angle distribution becomes obvious as the harmonic orders get farther and farther away from the
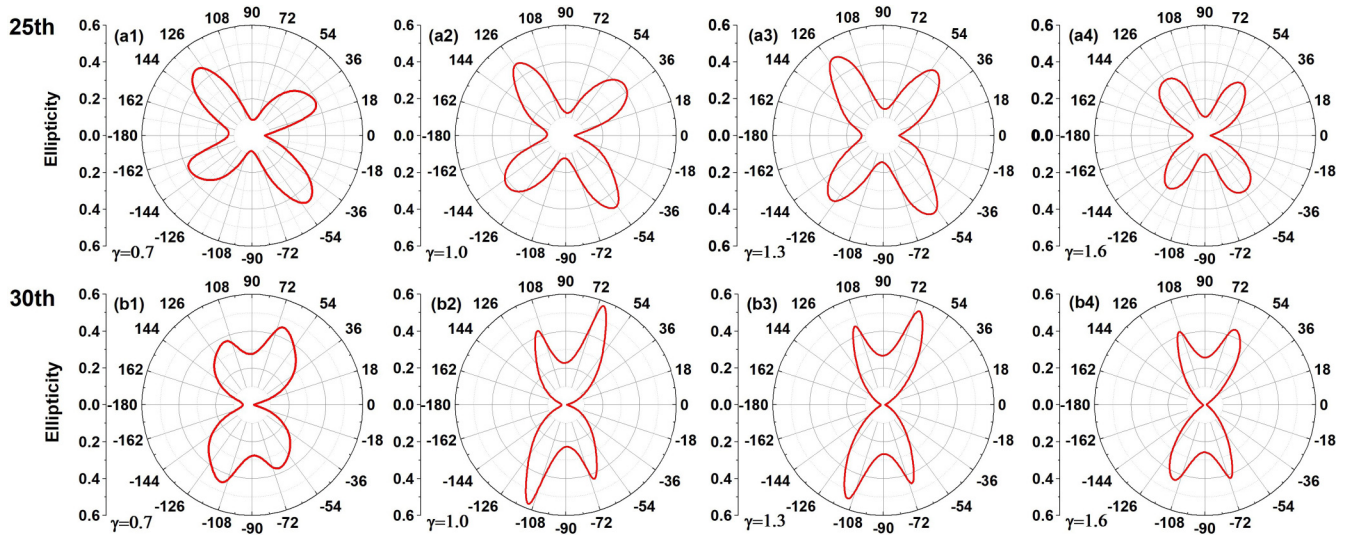
FIG. 4. Angular distribution of the ellipticity of the HHG for (a1)–(a4) 25th order and (b1)–(b4) 30th order with (a1),(b1) $\gamma = 0.7$, (a2),(b2) $\gamma = 1.0$, (a3),(b3) $\gamma = 1.3$, and (a4),(b4) $\gamma = 1.6$, respectively.

ionization threshold (we do not show the angular distribution of the ellipticity of these harmonic orders here).

To get a deeper insight of the ellipticity, we use the two-center interference effect on the harmonic spectrum to investigate the physical mechanism of the ellipticity of the harmonics. According to the previous work [30,33,34], the contributions of the harmonic generation from two nuclei can be separately investigated. The harmonic spectrum can be written as

$$|G(\omega)|^2 = |G_1(\omega)|^2 + |G_2(\omega)|^2 + 2 \, \text{Re} \, [G_1(\omega)G_2^*(\omega)],$$
(8)

where $G_j(\omega) = \int e^{i\omega t} \langle \psi(t)|\nabla V_j(r)|\psi(t)\rangle dt$, $j = 1, 2$. $|G_j(\omega)|^2$ can be regarded as the harmonic spectrum generated from nucleus j without considering another nucleus. It is clear that $|G(\omega)|^2$ is the total harmonic spectrum with the interference effect and $|G_1(\omega)|^2 + |G_2(\omega)|^2$ is the harmonic spectrum without the interference effect; $2 \, \text{Re}[G_1(\omega)G_2^*(\omega)]$ is the interference term from two nuclei.

Figure 5 presents the harmonic spectrum with and without the interference effect for four alignment angles $\theta = 0°, 72°, -54°, -72°$ with $\gamma = 1.6$, where $F_x(\omega)$ and $F_y(\omega)$ represent the x and y components of the harmonics with the interference effect, respectively, and $F_x'(\omega)$ and $F_y'(\omega)$ represent that without the interference effect, respectively. From Fig. 4 we can see that the ellipticities are small for 25th and 30th order harmonics with $\theta = 0°$, which can act as a contrast angle, the ellipticity is larger for 25th order harmonic with $\theta = -54°$, and the ellipticity is larger for 30th order harmonic with $\theta = \pm 72°$.

We can find that the odd-order harmonics in the x component are generated and the even-order harmonics in the y component are generated with the interference effect for $\theta = 0°$, as shown in Fig. 5(a). The odd-order harmonics in the x component are generated and the even-order harmonics and the weak odd-order harmonics in the y component are generated with the interference effect for $\theta = 72°$, as shown in Fig. 5(b).

The odd- and even-order harmonics in the x and y component are generated with the interference effect for $\theta = -54°$, as shown in Fig. 5(c). The odd- and even-order harmonics in the x component are generated and the even-order harmonics in the y component are generated with the interference effect for $\theta = -72°$, as shown in Fig. 5(d). This means that the parity of the HHG spectrum depends on the molecular alignment angle. Our results that the parity of the HHG depends on the molecular alignment angle for the H_2^+ molecule driven by the OTC laser field are consistent with the results of the CO molecule for different orientation angles driven by a linearly polarized laser field [45].

For $\theta = 0°$, the harmonic intensity in the x component with the interference effect is weaker than that without the interference effect; however, a reversed result can be obtained for the harmonics in the y component, as shown in Fig. 5(a). For $\theta = 72°$, the harmonic intensities in the x and y components with the interference effect are all weaker than that without the interference effect, as shown in Fig. 5(b). For $\theta = -54°, -72°$, the harmonic intensity in the y component with the interference effect is weaker than that without the interference effect, whereas the harmonic intensity in the x component with the interference effect and without the interference effect are comparable, as shown in Figs. 5(c) and 5(d).

From Fig. 5(a), we can find that the harmonic intensities for the x and y components with the interference effect for 25th order harmonic with $\theta = 0°$ are 1.14×10^{-9} and 5.76×10^{-9}, respectively, which differ by about 0.7 orders of magnitude. For 30th order harmonic, the harmonic intensities for the x and y components with the interference effect are 3.9×10^{-11} and 7.83×10^{-8}, respectively, which differ by about 3.3 orders of magnitude. Similarly, in Fig. 5(b), we can find that the harmonic intensities for the x and y components with the interference effect for 25th order harmonic with $\theta = 72°$ are 6.6×10^{-9} and 2.69×10^{-9}, respectively, which differ by about 0.39 orders of magnitude. For 30th order harmonic, the harmonic intensities for the x and y components with the interference effect are 3.5×10^{-9} and 1.29×10^{-8},
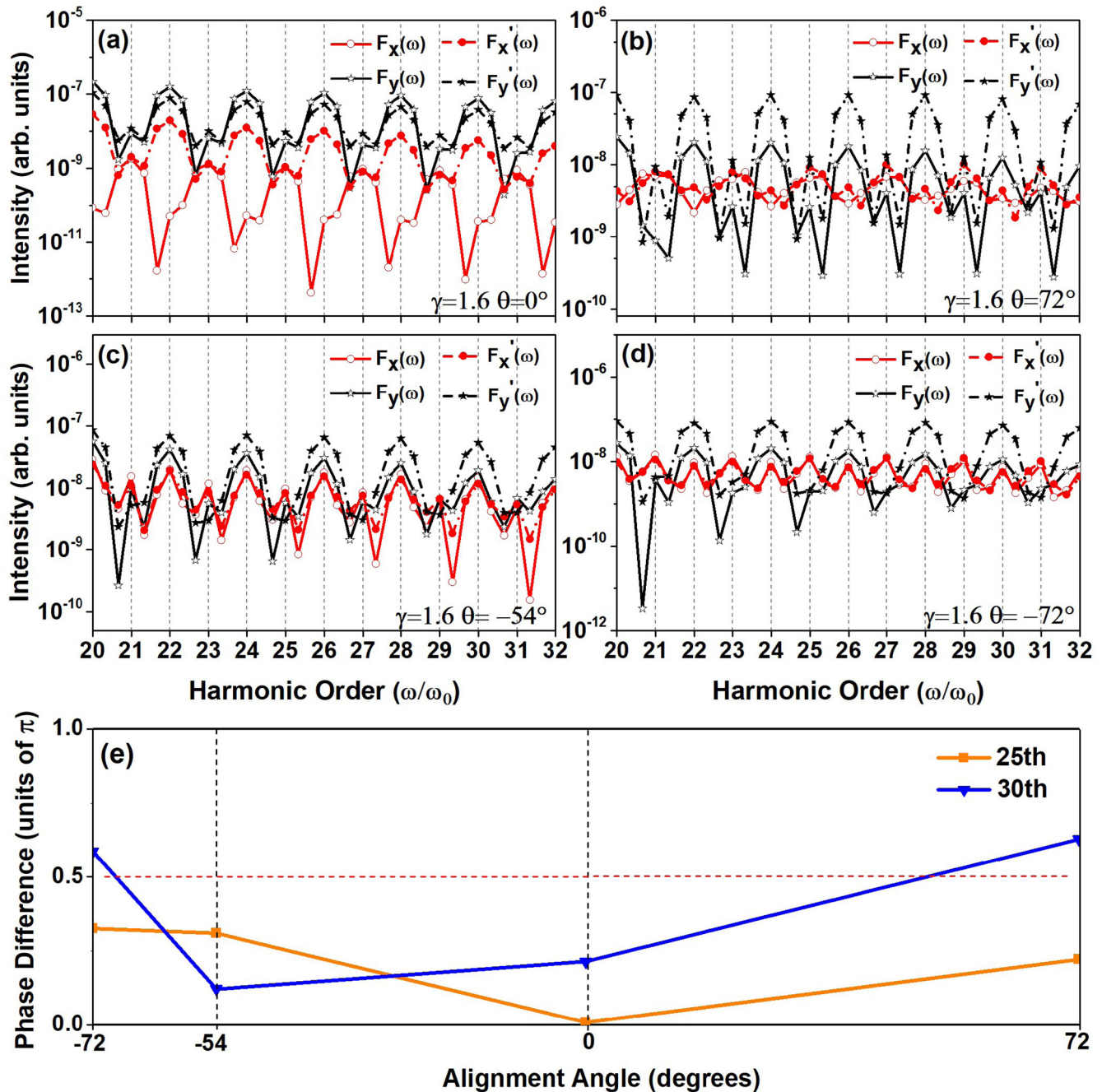
FIG. 5. Harmonic spectrum generated by the OTC laser field for four alignment angles: (a) $\theta = 0°$, (b) $\theta = 72°$, (c) $\theta = -54°$, and (d) $\theta = -72°$ with $\gamma = 1.6$, respectively. $F_x(\omega)$ and $F_y(\omega)$ represent the x and y components of the harmonics with the interference effect, respectively. $F_x'(\omega)$ and $F_y'(\omega)$ represent that without the interference effect, respectively. (e) The phase difference of 25th and 30th order harmonics for $\theta = 0°, 72°, -54°, -72°$ with $\gamma = 1.6$.

respectively, which differ by about 0.56 orders of magnitude. From Fig. 5(c), it can be found that the harmonic intensities for the x and y components with the interference effect for 25th order harmonic with $\theta = -54°$ are 9.9×10^{-9} and 6.01×10^{-9}, respectively, which differ by about 0.22 orders of magnitude. For 30th order harmonic, the harmonic intensities for the x and y components with the interference effect are 1.462×10^{-8} and 1.96×10^{-8}, respectively, which differ by about 0.127 orders of magnitude. From Fig. 5(d), it can be found that the harmonic intensities for the x and y com-

ponents with the interference effect for 25th order harmonic with $\theta = -72°$ are 1.408×10^{-8} and 2.09×10^{-9}, respectively, which differ by about 0.83 orders of magnitude. For 30th order harmonic, the harmonic intensities for the x and y components with the interference effect are 7.29×10^{-9} and 1.179×10^{-8}, respectively, which differ by about 0.21 orders of magnitude.

Obviously, the harmonic amplitude difference of the x and y components for 25th order harmonic with $\theta = -54°$ and that for 30th order harmonic with $\theta = \pm 72°$ are smaller than

that for 25th and 30th order harmonics with $\theta = 0°$, which results in the larger ellipticity for 25th order harmonic with $\theta = -54°$ and 30th order harmonic with $\pm72°$ than that of 25th and 30th order harmonics with $\theta = 0°$, which are consistent with that shown in Fig. 4(a4) and Fig. 4(b4), respectively.

In Fig. 5(e), we give the comparison of the phase difference for 25th and 30th order harmonics with $\theta = 0°, 72°, -54°, -72°$ to further illustrate the ellipticity. We can find that the phase difference with $\theta = -54°, \pm72°$ is closer to $\pi/2$ compared with that with $\theta = 0°$ for 25th order harmonic. Thus the ellipticity with $\theta = -54°, \pm72°$ is larger than that with $\theta = 0°$ for 25th order. The phase difference with $\theta = \pm72°$ is closer to $\pi/2$ compared with that with $\theta = 0°$ for 30th order harmonic. Thus the ellipticity with $\theta = \pm72°$ is larger than that with $\theta = 0°$ for 30th order harmonic, which are consistent with that described above. Even if the phase difference with $\theta = 0°$ is closer to $\pi/2$ than that with $\theta = -54°$ for 30th order harmonic, the amplitude difference for the x and y components of the harmonics with $\theta = 0°$ is much larger than that with $\theta = -54°$; thus the ellipticity with $\theta = -54°$ is larger than that with $\theta = 0°$ for 30th order harmonic.

The phase differences with $\theta = -54°, -72°$ for 25th order harmonic are comparable; however, the amplitude difference for the x and y components of the harmonics with $\theta = -54°$ is smaller than that with $\theta = -72°$, which results in the smaller ellipticity with $\theta = -72°$ compared with that with $\theta = -54°$. The phase differences with $\theta = -54°, -72°$ for 25th order harmonic are closer to $\pi/2$ than that with $\theta = 72°$, which results in the larger ellipticity with $\theta = -54°, -72°$ compared with that with $\theta = 72°$. Similarly, for 30th order harmonic, the phase difference with $\theta = -54°$ is farther away from $\pi/2$ than that of $\theta = \pm72°$, which results in the smaller ellipticity with $\theta = -54°$ compared with that with $\theta = \pm72°$, which are consistent with the results shown in Figs. 4(a4) and 4(b4).

In Figs. 5(a)–5(d), we give the x and y components of the harmonics without the interference effect to illustrate the dependence of the ellipticity on the interference effect. The influence of the interference effect on the ellipticity can be reflected by the amplitude difference of the x and y components of the harmonics.

From Fig. 5(a), we can find that the harmonic intensities for the x and y components without the interference effect for 25th order harmonic with $\theta = 0°$ are 8.27×10^{-10} and 1.12×10^{-8}, respectively, which differ by about 1.13 orders of magnitude. For 30th order harmonic, the harmonic intensities in the x and y components without the interference effect are 5.21×10^{-9} and 4.17×10^{-8}, respectively, which differ by about 0.9 orders of magnitude. In Fig. 5(b), we can find that the harmonic intensities for the x and y components without the interference effect for 25th order harmonic with $\theta = 72°$ are 9.02×10^{-9} and 1.29×10^{-8}, respectively, which differ by about 0.15 orders of magnitude. For 30th order harmonic, the harmonic intensities in the x and y components without

the interference effect are 4.34×10^{-9} and 7.7×10^{-8}, respectively, which differ by about 1.24 orders of magnitude. In Fig. 5(c), we can find that the harmonic intensities for the x and y components without the interference effect for 25th order harmonic with $\theta = -54°$ are 8.4×10^{-9} and 2.88×10^{-9}, respectively, which differ by about 0.46 orders of magnitude. For 30th order harmonic, the harmonic intensities in the x and y components without the interference effect are 1.25×10^{-8} and 5.72×10^{-8}, respectively, which differ by about 0.66 orders of magnitude. In Fig. 5(d), we can find that the harmonic intensities for the x and y components without the interference effect for 25th order harmonic with $\theta = -72°$ are 1.28×10^{-8} and 1.72×10^{-9}, respectively, which differ by about 0.87 orders of magnitude. For 30th order harmonic, the harmonic intensities in the x and y components without the interference effect are 5.99×10^{-9} and 7.23×10^{-8}, respectively, which differ by about 1.08 orders of magnitude.

Obviously, the amplitude ratio in the x and y components of the harmonics without the interference effect are different from that with the interference effect. These mean that the two-center interference effect can affect the amplitude difference of the x and y components of the harmonics and further affect the ellipticity of the harmonics.

IV. CONCLUSIONS

In conclusion, we investigated the ellipticity of the HHG for the H_2^+ molecule at different intensity ratios $\gamma = 0.7, 1.0, 1.3, 1.6$ driven by the OTC laser field through numerically solving the 2D TDSE. We find that the odd-order harmonics in the x component and the even-order harmonics in the y component can be generated with the specific alignment angle $\theta = 0°$ and the physical mechanism can be illustrated by the quantum transition. The ellipticity can be controlled by adjusting the intensity ratio of the laser fields and alignment angles. The phase difference of the x and y components of the harmonics with $\theta = -54°$ is investigated to illustrate the general physical mechanism of the ellipticity. The results show that the ellipticity is larger around $\pm\pi/2$ than that around 0 or $\pm\pi$. Subsequently, we show that the ellipticity of the harmonics varies with the harmonic orders and the alignment angles. And the intensity ratio has little effect on the angular distribution of the ellipticity for particular harmonic order. We further present the harmonic spectrum with and without the interference effect. The results show that the two-center interference effect can affect the amplitude difference of the x and y components of the harmonics and further affect the ellipticity of the harmonics.

[1] X.-L. Ge, H. Du, J. Guo, and X.-S. Liu, Opt. Express **23**, 8837 (2015).

[2] M. Qin and X. Zhu, Opt. Laser Technol. **87**, 79 (2017).

[3] J. Itatani, J. Levesque, D. Zeidler, H. Niikura, H. Pépin, J. C. Kieffer, P. B. Corkum, and D. M. Villeneuve, Nature (London) **432**, 867 (2004).

[4] Y. Mairesse, A. de Bohan, L. J. Frasinski, H. Merdji, L. C. Dinu, P. Monchicourt, P. Breger, M. Kovačev, R. Taïeb, B. Carré, H. G. Muller, P. Agostini, and P. Salières, Science **302**, 1540 (2003).

[5] P. B. Corkum, Phys. Rev. Lett. **71**, 1994 (1993).

[6] D. Wang, X. Zhu, H. Yuan, P. Lan, and P. Lu, Phys. Rev. A **101**, 023406 (2020).

[7] J. Zhang, X.-X. Huo, T. Qi, J. Guo, and X.-S. Liu, Laser Phys. **30**, 045302 (2020).

[8] K.-J. Yuan and A. D. Bandrauk, Phys. Rev. A **100**, 033420 (2019).

[9] C. Zhai, R. Shao, P. Lan, B. Wang, Y. Zhang, H. Yuan, S. M. Njoroge, L. He, and P. Lu, Phys. Rev. A **101**, 053407 (2020).

[10] S. Yu, B. Zhang, Y. Li, S. Yang, and Y. Chen, Phys. Rev. A **90**, 053844 (2014).

[11] X. Zhou, R. Lock, N. Wagner, W. Li, H. C. Kapteyn, and M. M. Murnane, Phys. Rev. Lett. **102**, 073902 (2009).

[12] L. Barreau, K. Veyrinas, V. Gruson, S. J. Weber, T. Auguste, J.-F. Hergott, F. Lepetit, B. Carré, J.-C. Houver, D. Dowek, and P. Salières, Nat. Commun. **9**, 4727 (2018).

[13] K.-J. Yuan and A. D. Bandrauk, Phys. Rev. A **81**, 063412 (2010).

[14] H. Yang, P. Liu, R. Li, and Z. Xu, Opt. Express **21**, 28676 (2013).

[15] G. Lambert, B. Vodungbo, J. Gautier, B. Mahieu, V. Malka, S. Sebban, P. Zeitoun, J. Luning, J. Perron, A. Andreev, S. Stremoukhov, F. Ardana-Lamas, A. Dax, C. P. Hauri, A. Sardinha, and M. Fajardo, Nat. Commun. **6**, 6167 (2015).

[16] D. Habibović and D. B. Milošević, Photonics **7**, 110 (2020).

[17] D. B. Milošević and W. Becker, Phys. Rev. A **100**, 031401(R) (2019).

[18] S. Stremoukhov, A. Andreev, B. Vodungbo, P. Salières, B. Mahieu, and G. Lambert, Phys. Rev. A **94**, 013855 (2016).

[19] S.-K. Son, D. A. Telnov, and S.-I. Chu, Phys. Rev. A **82**, 043829 (2010).

[20] S. Ramakrishna, P. A. J. Sherratt, A. D. Dutoi, and T. Seideman, Phys. Rev. A **81**, 021802(R) (2010).

[21] P. A. J. Sherratt, S. Ramakrishna, and T. Seideman, Phys. Rev. A **83**, 053425 (2011).

[22] A. Etches, C. B. Madsen, and L. B. Madsen, Phys. Rev. A **81**, 013409 (2010).

[23] X. Zhang, X. Zhu, X. Liu, D. Wang, Q. Zhang, P. Lan, and P. Lu, Opt. Lett. **42**, 1027 (2017).

[24] B. Mahieu, S. Stremoukhov, D. Gauthier, C. Spezzani, C. Alves, B. Vodungbo, P. Zeitoun, V. Malka, G. De Ninno, and G. Lambert, Phys. Rev. A **97**, 043857 (2018).

[25] Y. Mairesse, J. Higuet, N. Dudovich, D. Shafir, B. Fabre, E. Mével, E. Constant, S. Patchkovskii, Z. Walters, M. Y. Ivanov, and O. Smirnova, Phys. Rev. Lett. **104**, 213601 (2010).

[26] M.-Z. Li, Y. Xu, G.-R. Jia, and X.-B. Bian, Phys. Rev. A **100**, 033410 (2019).

[27] F. Dong, Y. Tian, S. Yu, S. Wang, S. Yang, and Y. Chen, Opt. Express **23**, 18106 (2015).

[28] M. Lein, N. Hay, R. Velotta, J. P. Marangos, and P. L. Knight, Phys. Rev. A **66**, 023805 (2002).

[29] M. Lein, N. Hay, R. Velotta, J. P. Marangos, and P. L. Knight, Phys. Rev. Lett. **88**, 183903 (2002).

[30] G. L. Kamta and A. D. Bandrauk, Phys. Rev. A **71**, 053407 (2005).

[31] D. A. Telnov and S.-I. Chu, Phys. Rev. A **76**, 043412 (2007).

[32] J. Zhang, X.-L. Ge, T. Wang, T.-T. Xu, J. Guo, and X.-S. Liu, Phys. Rev. A **92**, 013418 (2015).

[33] C. Yu, S. C. Jiang, X. Cao, G. L. Yuan, T. Wu, L. H. Bai, and R. F. Lu, Opt. Express **24**, 19736 (2016).

[34] H.-R. Li, H.-D. Zhang, J. Zhang, X.-F. Pan, P.-Y. Guo, and X.-S. Liu, Opt. Commun. **436**, 121 (2019).

[35] T. Das and C. Figueira de Morisson Faria, Phys. Rev. A **94**, 023406 (2016).

[36] V. V. Kim, R. A. Ganeev, G. S. Boltaev, and A. S. Alnaser, J. Phys. B: At., Mol., Opt. Phys. **53**, 155405 (2020).

[37] E. V. van der Zwan and M. Lein, Phys. Rev. A **82**, 033405 (2010).

[38] B. Zhang and M. Lein, Phys. Rev. A **100**, 043401 (2019).

[39] F. He, C. Ruiz, and A. Becker, Phys. Rev. A **75**, 053407 (2007).

[40] J. B. Bertrand, H. J. Wörner, H.-C. Bandulet, É. Bisson, M. Spanner, J.-C. Kieffer, D. M. Villeneuve, and P. B. Corkum, Phys. Rev. Lett. **106**, 023001 (2011).

[41] M. D. Perry and J. K. Crane, Phys. Rev. A **48**, R4051 (1993).

[42] E. Pisanty, S. Sukiasyan, and M. Ivanov, Phys. Rev. A **90**, 043829 (2014).

[43] A. Fleischer and N. Moiseyev, Phys. Rev. A **74**, 053806 (2006).

[44] O. Smirnova, S. Patchkovskii, Y. Mairesse, N. Dudovich, D. Villeneuve, P. Corkum, and M. Y. Ivanov, Phys. Rev. Lett. **102**, 063601 (2009).

[45] N.-L. Phan, C.-T. Le, V.-H. Hoang, and V.-H. Le, Phys. Chem. Chem. Phys. **21**, 24177 (2019).